Cell Reports
Physical Science

CellPress
OPEN ACCESS

Report

A dynamic wall design with tunable angular emissivity for all-season thermal regulation

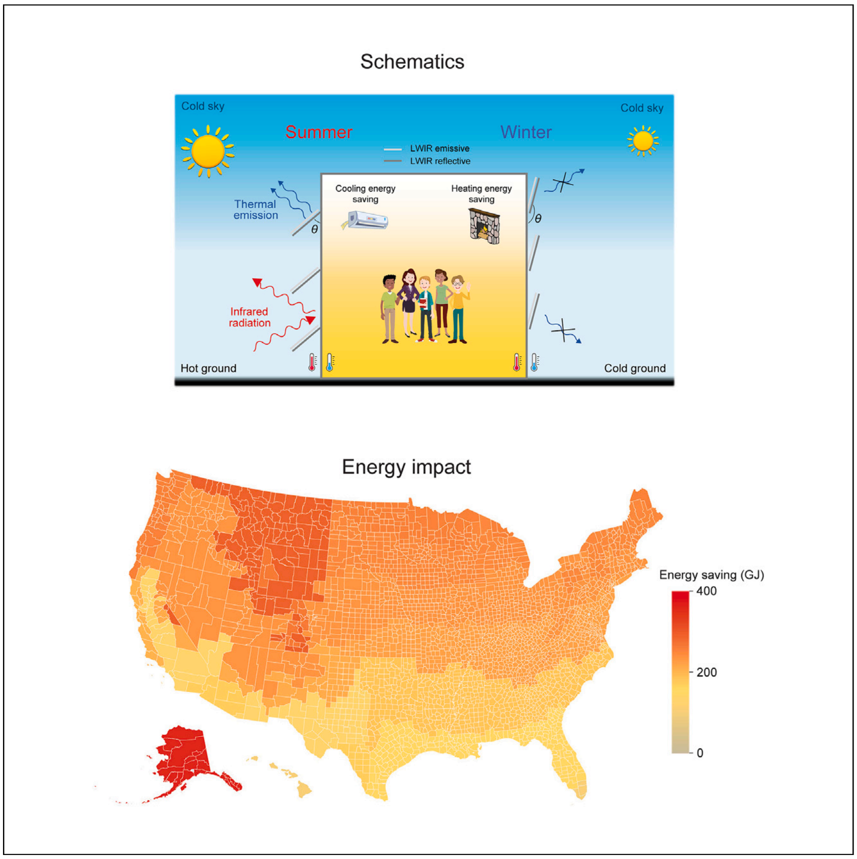

In the building envelope, current radiative cooling walls save cooling energy in the summer but induce a "heating penalty" in the winter. To overcome this issue, Cheng et al. introduce and validate a scalable wall design with tunable angular emissivity. It enables all-season thermal regulation and reduces building energy consumption.

Qilong Cheng, Chao Tang, Dianlun Luo, Minjoon Park, Steven Tian, Yuan Yang

yy2664@columbia.edu

Highlights

A scalable FinWall design is proposed to achieve tunable angular emissivity

This FinWall design enables all-season thermal regulation for building walls

The FinWalls can save 24% annual energy versus high-emissivity walls in the US

Cheng et al., Cell Reports Physical Science 5, 101934
May 15, 2024
https://doi.org/10.1016/j.xcrp.2024.101934

Cell Reports
Physical Science

CellPress
OPEN ACCESS

Report

A dynamic wall design with tunable angular emissivity for all-season thermal regulation

Qilong Cheng,[1] Chao Tang,[2] Dianlun Luo,[3] Minjoon Park,[4] Steven Tian,[2] and Yuan Yang[1,5,*]

SUMMARY

Radiative cooling achieves passive cooling by emitting long-wavelength infrared radiation (LWIR) to outer space. Increasing attention has been paid to radiative cooling walls in the building envelope. However, its undesired cooling effect in the winter exacerbates the heating demand of buildings. Here, we report a scalable wall design with dynamic rotatable fins (FinWall) to achieve tunable angular LWIR emissivity on the wall surface, enabling all-season thermal regulation. Field tests demonstrate that the FinWall yields a $\sim$2.0°C temperature elevation under cold weather and a $\sim$3.1°C temperature drop under hot weather compared to conventional high LWIR emissivity walls. This translates to extra power savings of 37 W m^{-2} for heating and 53 W m^{-2} for cooling. Further building simulations indicate that a mid-rise apartment building equipped with FinWalls can save 24% (or 10%) annual energy versus the same building with high-emissivity walls (or low-emissivity walls) in the US.

INTRODUCTION

With carbon peak and carbon neutrality goals, the utilization and regulation of energy have emerged as pivotal steps to establish an energy-efficient and environmentally friendly society.[1] Among human activities, buildings is the most energy-consuming sector, responsible for approximately 40% of global energy and 36% of CO_2 emissions.[2] In particular, space cooling technologies including fans and air conditioners use more than 2,000 TWh of electricity per year, and this value is estimated to triple by 2050 due to the growing cooling demand.[3] Therefore, an electricity-free cooling approach, radiative cooling, has drawn increasing attention for energy savings in the buildings sector. It achieves passive cooling by emitting long-wavelength infrared radiation (LWIR) to outer space through an atmospheric transparency window that ranges from wavelengths of 8 to 13 μm.[4] This radiative heat exchange can naturally cool the surfaces of certain objects by several degrees Celsius below the ambient air temperature,[5–9] a phenomenon known as sub-ambient radiative cooling. Thus, radiative cooling can be applied in multiple scenarios with access to the sky and outer space, such as building rooftops,[10,11] greenhouses,[12] vehicles,[13,14] and personal textiles,[15,16] to achieve thermal regulation.

Radiative cooling has been successfully and broadly demonstrated on building rooftops because the roof surface exhibits the most pronounced cooling effect, since its view factor to the sky is close to unity. Furthermore, recently, researchers started to explore radiative cooling for vertical walls either by an angle-selective emitter[17,18] or

[1]Department of Applied Physics and Applied Mathematics, Columbia University, New York, NY 10027, USA
[2]Department of Mechanical Engineering, Columbia University, New York, NY 10027, USA
[3]Department of Mathematics, Columbia University, New York, NY 10027, USA
[4]Korea International School, Seongnam-si, Gyeonggi-do 13543, South Korea
[5]Lead contact
*Correspondence: yy2664@columbia.edu
https://doi.org/10.1016/j.xcrp.2024.101934

by a wavelength-selective emitter.[19] However, these emitters still radiate thermal radiation in the cold seasons and further reduce the temperature. Such undesired cooling exacerbates the heating demand of buildings and escalates energy consumption, which is also known as the "heating penalty."[20] Considering that the vast majority of the human population resides in temperature zones with distinct seasons,[21] addressing the heating penalty issue is crucial to significantly advancing the practical implementation of radiative cooling.

Several strategies have been proposed to address the heating penalty issue, including thermochromism, electrochromism, reconfigurable mechanical structures, and wetting-responsive structures. Vanadium dioxide (VO_2)-based materials make up a well-known thermochromic family featuring emissivity change along with metal-insulator transition.[22–24] They exhibit high LWIR emissivity (high-E) at high temperatures for radiative cooling but low LWIR emissivity (low-E) at low temperatures to deactivate radiative cooling and mitigate the heating penalty. Electrochromic designs can also achieve a high-emissivity state as a cooling mode and a low-emissivity state as a heating mode via lithium ion intercalation[25] or reversible metal electrodeposition.[26] In addition to designing new materials, various structures can utilize commercially available inexpensive materials to tune optical properties and provide simple environmentally friendly solutions. Examples include reconfigurable louvers,[27] Kirigami structures,[28] strain-driven photonic structure,[29] and wetting-responsive polymers.[30] However, these strategies typically involve two states or multiple intermediate states with uniform angular emissivity, rendering them unsuitable for all-season thermally regulated walls, as angularly isotropic emitters are not the optimal solution.[17,18]

Here, we present a scalable and well-controllable wall design with dynamic rotatable fins (FinWall) to achieve tunable angular LWIR emissivity of the wall surface enabling all-season thermal regulation (Figure 1A). The top and bottom surfaces of the fins are coated with high-E materials and low-E materials, respectively. The vertical wall surface remains low-E. In the summer, with the ground surface temperature around 50°C–60°C, the FinWall surface exhibits high-E when facing the cold sky and low-E when facing the hot ground (Figure 1A, left). This angular asymmetric emissivity ensures simultaneous radiative cooling to the sky and reflection of thermal radiation from the hot ground, resulting in optimal cooling compared to flat walls with isotropic high-E or low-E materials. In the winter, the FinWall surface remains low-E toward the outside by rotating the fins to a certain angle ($\theta \rightarrow 180^\circ$; Figure 1A, right). In this way, the FinWall operates in the heating mode by cutting off radiation loss to the sky or cold ground.

Figure 1B illustrates the ideal angular emissivity profiles alongside the simulated angular emissivity of the FinWall in both the cooling mode and the heating mode (Note S1). In the cooling mode ($\theta = 45^\circ$), the simulated emissivity closely matches the ideal black dashed curve at all angles, except that the transition between $\sim 20^\circ$ and -45° is gradual. This deviation does not compromise the FinWall performance substantially for two reasons: (1) radiative cooling is much less effective near the horizon ($\varphi = \sim 20^\circ$–0°) due to a larger air mass and (2) the ground surface near the horizon ($\varphi = 0^\circ$ to -45°) is distant from the FinWall, and this region contributes a smaller radiation component to the FinWall, following Lambert's cosine law. In the heating mode ($\theta = 165^\circ$), the simulated FinWall emissivity aligns well with the ideal red dashed curve. Consequently, the FinWall can seamlessly transition between the cooling mode and the heating mode by adjusting the fin orientation.

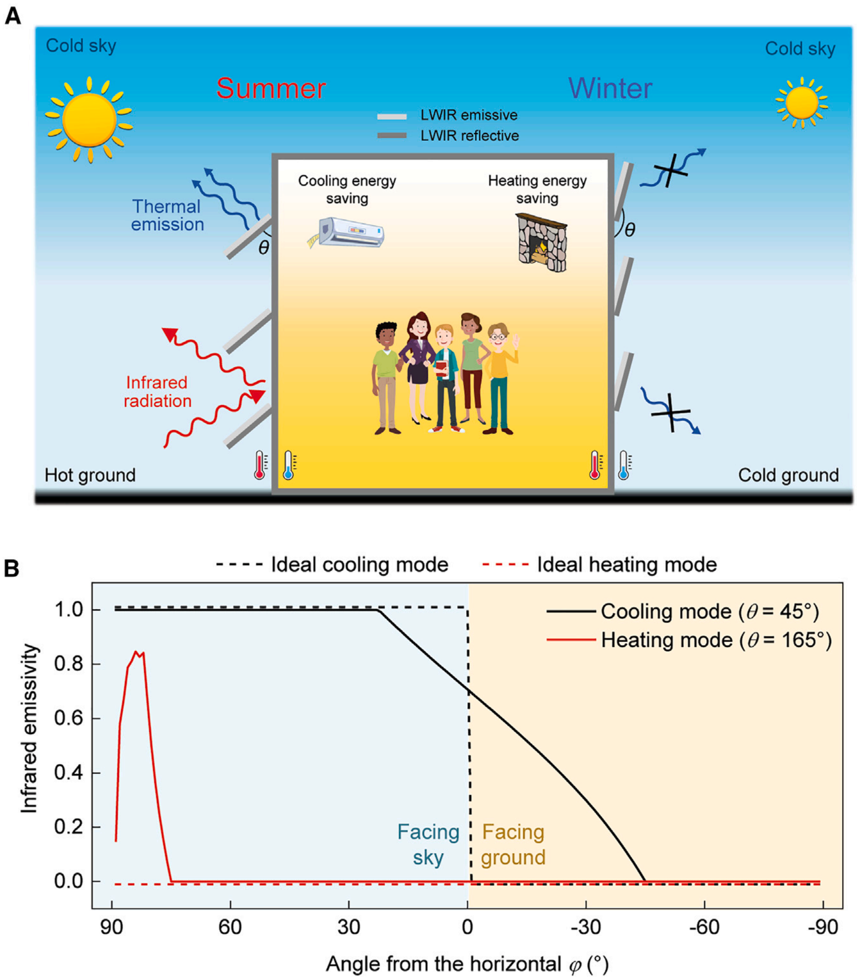

Figure 1. Concept illustration

(A) The fins, consisting of LWIR emissive and reflective surfaces, are designed to achieve all-season thermal regulation for building walls.

(B) The ideal angular LWIR emissivity for cooling mode and heating mode, along with simulated FinWall emissivity. In the FinWall, the emissive surface is an ideal LWIR emitter (emissivity $\varepsilon = 1$), and the reflective surface is an ideal LWIR reflector ($\varepsilon = 0$).

RESULTS

Theoretical power savings of FinWalls

To comprehend and optimize the energy-saving potential of the FinWall design, thermal simulations were first conducted to explore its theoretical capabilities (Note S2). The baseline case is a plain isotropic high-E wall. Its heat exchange with the surroundings (sun, sky, ground, air) was calculated, and a baseline cooler (or heater) power $P_{\text{cooler, high-E}}$ (or $P_{\text{heater, high-E}}$) was determined to maintain itself at 20°C in the summer (or winter). On the other hand, the $P_{\text{cooler, FinWall}}$ (or $P_{\text{heater, FinWall}}$) required by the FinWall in the cooling (or heating) mode was computed and compared with the baseline high-E values. The difference $P_{\text{cooler, high-E}} - P_{\text{cooler, FinWall}}$ (or $P_{\text{heater, high-E}} - P_{\text{heater, FinWall}}$) is defined as the saved cooling power $P_{\text{cool, save}}$ (or saved heating power $P_{\text{heat, save}}$) in the summer (or winter) (Figure S2).

First, it is observed that high specularity enhances power savings of FinWalls. Figures 2A–2D clearly demonstrate that the FinWall with specularly reflective

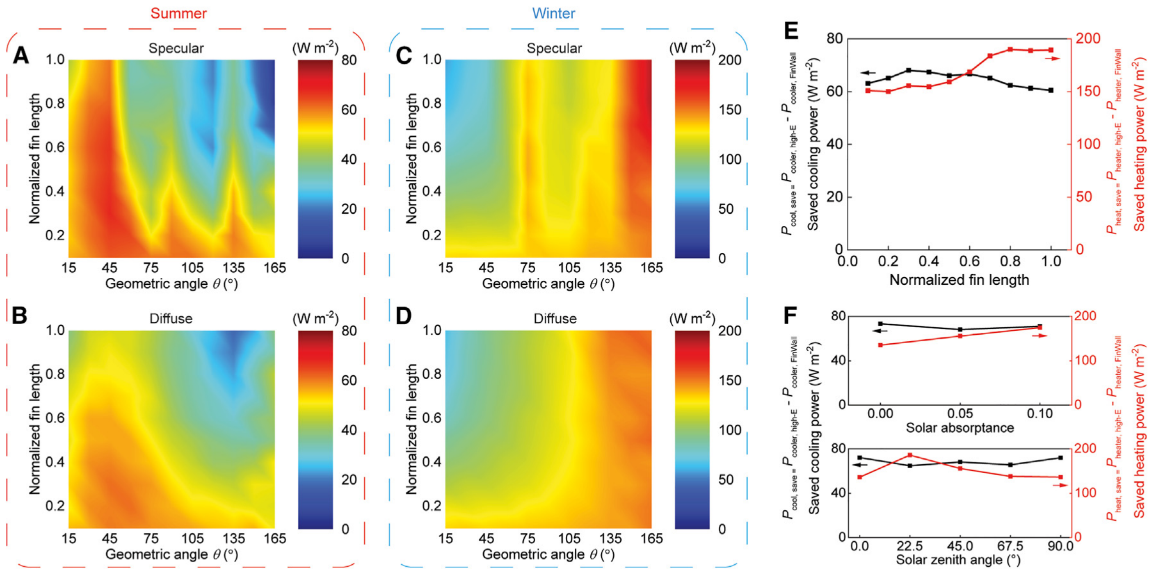

Figure 2. Simulation of power savings of dynamic FinWalls

(A and B) Contour mappings depicting saved cooling power ($P_{cool,\ save} = P_{cooler,\ high\text{-}E} - P_{cooler,\ FinWall}$) over the fin geometric angle θ and normalized fin length, with the fin surfaces being specularly reflective (A) or diffusely reflective (B). Normalized fin length is defined as the ratio between the fin length and the period between fins.

(C and D) Contour mappings depicting saved heating power ($P_{heat,\ save} = P_{heater,\ high\text{-}E} - P_{heater,\ FinWall}$) over the fin geometric angle θ and the normalized fin length for the specular case (C) and the diffuse case (D). The absolute values of $P_{cooler,\ high\text{-}E}$, $P_{cooler,\ FinWall}$, $P_{heater,\ high\text{-}E}$, and $P_{heater,\ FinWall}$ are presented in Figure S4.

(E) Angle-optimized $P_{cool,\ save}$ and $P_{heat,\ save}$ as a function of normalized fin length.

(F) Effects of solar absorptance and solar zenith angle on $P_{cool,\ save}$ and $P_{heat,\ save}$.

The ground surface temperature is set at 60°C for the summer case (A and B) and 0°C for the winter case (C and D). In (A)–(D), the FinWall consists of ideal LWIR emitters (ε = 1) and ideal LWIR reflectors (ε = 0) with a solar absorptance of 0.05, and the solar zenith angle is 45°. In (F), the normalized fin length is chosen to be 0.3.

surfaces can achieve greater power savings than one with diffusely reflective surfaces in both summer and winter. In the summer, the specular FinWall shows a maximized saved cooling power of 68 W m^{-2}, compared to 61 W m^{-2} for the diffuse FinWall, at an optimal geometric angle θ of 45° (cooling mode). Similarly, the specular FinWall exhibits a maximized saved heating power of 190 W m^{-2} at θ = 165° (heating mode), which is much higher than 155 W m^{-2} for the diffuse FinWall. This is attributed to the multiple reflections occurring among different surfaces of the FinWall. Specularity effectively reduces multiple reflections, thus lowering solar or LWIR absorption in the summer to provide more cooling or reducing radiation loss in the winter to offer more heating (Figure S3). To maintain high specularity, mirror-like aluminized mylar film and solar-transparent polydimethylsiloxane (PDMS) were chosen as the LWIR reflective and emissive surfaces of the FinWall.

The angle-optimized power savings are derived from Figures 2A and 2C and plotted in Figure 2E as a function of the normalized fin length. For cooling purposes, a normalized fin length of 0.3 yields an optimal saved cooling power of 68 W m^{-2}. The dependence of the saved cooling power on the fin length does not align with the principle in heat convection that longer is better because longer fins would obstruct each other and impede radiative cooling to the sky. Moreover, longer fins would lead to an extended heat conduction pathway from the fin surfaces to the vertical wall itself and a larger heat convection, compromising the cooling power obtained at the vertical wall. On the contrary, longer fins contribute to higher saved heating power in the winter case, as they can better conceal the emissive surfaces,

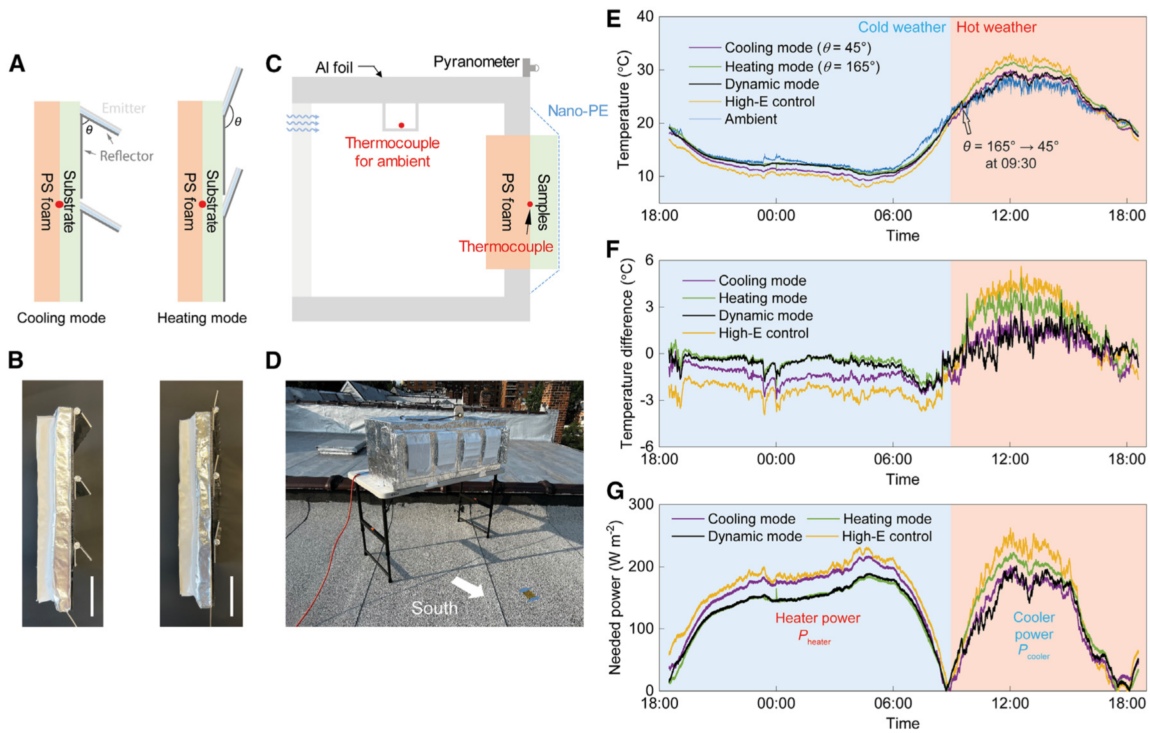

Figure 3. Experimental demonstration of dynamic FinWalls

(A) Schematics of a FinWall in the cooling mode and the heating mode.

(B) Side views of FinWall samples in the cooling mode and the heating mode. Scale bar: 3 cm.

(C) Schematic of the experimental setup. The FinWall samples are covered with nanoporous polyethylene (NanoPE; Figure S5) to maintain the same solar reflectance. The interior of the box is hollow, allowing the inside thermocouple to be under natural air flow and measure ambient air temperature.

(D) The experimental setup for field tests in Queens, New York, USA. The FinWall samples face south with solar irradiance up to ~840 W m^{-2} (Figure S6).

(E and F) Temperature variation (E) and temperature difference between a wall and the ambient (F) for four samples over a continuous 24 h.

(G) The calculated heater/cooler power to maintain the wall samples at 20°C. Two samples are fixed at the cooling mode (θ = 45°) and the heating mode (θ = 165°), respectively. The dynamic mode FinWall sample switched from the heating mode to the cooling mode at 09:30. The control sample is an isotropic high-E emitter.

approximating a low-E appearance. Taking material savings into account, a normalized fin length of 0.3 is chosen in Figure 2F and the following field tests. Figure 2F illustrates the versatility of FinWalls under varying degrees of solar absorption and different solar positions.

Experimental demonstration of FinWalls

To experimentally demonstrate all-season thermal regulation via the FinWall design, FinWall samples were prepared and are shown in Figures 3A and 3B. The FinWall samples have dimensions of 15 × 15 cm, with three fins of ~1.5 cm long and a fin period of 5 cm, so the normalized fin length is 0.3. Subsequently, the FinWall samples along with an isotropic high-E control were mounted on a box for field tests. In this study, the focus is on thermal regulation at LWIR wavelengths rather than solar wavelengths. Therefore, nanoporous polyethylene (NanoPE) was used as a cover over the samples (Figures 3C and 3D). NanoPE not only blocks sunlight due to its white appearance with a solar reflectance of 0.82 (Figure S5B) but also allows LWIR to pass through without absorption or scattering owing to its high LWIR specular transmittance (Figure S5C). Meanwhile, the diffuse appearance of NanoPE in the visible wavelengths also addresses the potential light pollution issue induced by specularly reflective surfaces in the FinWall.

A full-day field test was conducted in spring 2023 in Queens, New York, USA. As shown in Figure 3E, the ambient air temperature T_{amb} remained below 20.0°C from 18:30 to 09:00 and subsequently rose above 20.0°C. The ground surface temperature T_{ground} ranged from 6.2°C at 05:00 to 60.6°C at 13:30 (Figure S6). Therefore, 18:30–09:00 was used to mimic cold weather and 09:00–18:00 was used to mimic hot weather, as indicated by the shaded regions in Figure 3E. Four samples were tested: a FinWall in the cooling mode (θ = 45°), a FinWall in the heating mode (θ = 165°), a FinWall in the dynamic mode, and a high-E wall. To address different weather conditions, the dynamic mode FinWall switched from heating mode to cooling mode by rotating the joints between the wall and the fins.

Under the cold weather condition (18:30–09:00 in Figures 3E and 3F), the FinWalls in the heating mode and the dynamic mode both exhibit small temperature drops of ~0.4°C–0.5°C lower than T_{amb}, as their surfaces have low emissivity and thus present little radiative cooling. The FinWall in the cooling mode shows an average temperature drop of 1.4°C due to radiative cooling from its exposed emissive surfaces. The high-E wall, representing a common scenario in real building walls, displays the largest temperature drop of 2.4°C because the isotropic high-E surface not only loses radiative heat to the sky but also loses some heat to the cold ground. Therefore, the dynamic mode (or heating mode) results in a ~2.0°C temperature elevation compared to the conventional high-E case under cold weather, potentially reducing the energy reliance on heating units.

Under the hot weather condition with T_{ground} approaching 60°C (09:00–18:00 in Figures 3E and 3F), the FinWalls in the cooling mode and the dynamic mode both exhibit the smallest temperature rises (~0.8°C) compared to T_{amb} because they simultaneously maintain radiative cooling to the sky and reflect LWIR from the hot ground. The FinWall in the heating mode has a low-E appearance that does not emit LWIR to the surroundings, so it is heated to ~3.0°C above T_{amb} on average by a small amount of sunlight passing through the NanoPE cover. In the case of the high-E wall, it receives more LWIR radiation from the hot ground than radiative loss to the cold sky, resulting in a temperature rise of ~3.9°C at 10:00-15:00. Consequently, the dynamic FinWall in the cooling mode achieves a ~3.1°C drop under such a hot weather condition, which can reduce the energy consumption of cooling units substantially.

Furthermore, to quantify the power savings in terms of a heating/cooling unit, an imaginary heater/cooler is assumed to work under cold/hot weather conditions to maintain the wall samples at 20°C. The power needed for the heater (P_{heater}) or the cooler (P_{cooler}) is calculated analytically from the temperature data (Note S3) and plotted in Figure 3G. Under the cold weather condition, the dynamic FinWall in the heating mode only requires a heating power that is 28–48 W m^{-2} smaller than the high-E wall, and the average saved heating power is 37 W m^{-2}. Similarly, the dynamic FinWall in the cooling mode exhibits the smallest temperature rise under hot weather in Figure 3F, and thus it needs the smallest cooler power, as shown in Figure 3G. The resultant saved cooler power is 53 W m^{-2} on average at 10:00–15:00. Therefore, the field tests successfully demonstrated the FinWall's capability of all-season thermal regulation (2.0°C hotter in winter and 3.1°C cooler in summer than a conventional high-E wall), along with the reduction of the thermal loads in wall thermal management (37 W m^{-2} less heating in winter and 53 W m^{-2} less cooling in summer than a conventional high-E wall).

It is worth noting that the conventional fin effect to enhance heat convection due to extended surface area does not contribute to the power savings in either cooling

($P_{cool,\ save}$) or heating ($P_{heat,\ save}$) but instead reduces these values. Taking the winter as an example, when heated up to a reference temperature (e.g., 20°C) by a heating unit, more power would be dissipated as convection for a FinWall due to its extended surface area, as compared to a high-E wall. The same principle also applies to the cooling case in summer. Therefore, the convective heat exchange actually weakens the FinWall's heating capability in winter and its cooling capability in summer in comparison with the high-E wall. The FinWall's thermal regulation capability indeed stems from its ability to adjust radiative heat exchange with the surroundings. Detailed analyses can be found in Note S4 and Figure S9.

Energy impact of FinWalls

The prior simulation and experimental demonstrations of the FinWall performance focused solely on the heat exchange of the dynamic FinWall with outside surroundings, without considering the thermal mass and heat conduction of the walls themselves. Here, to investigate the building-scale energy impact of FinWalls in different climate zones, EnergyPlus simulations were conducted to calculate the annual energy consumption for heating, cooling, and fan, which takes heat conduction inside walls and the wall/building interaction into account. As an illustration, a post-1980 mid-rise apartment building, selected from the commercial reference buildings developed by the US Department of Energy (DOE), is used. This reference assumes different insulation thicknesses in the building walls, with the total wall thermal resistance varying from 0.2 $m^2\ K\ W^{-1}$ in warm areas to 3.8 $m^2\ K\ W^{-1}$ in cold areas, which are standard values provided by the DOE (Note S5). The mid-rise apartment building is modified to integrate with dynamic FinWalls (Figure 4A), while all other features such as windows, doors, and thermal settings remain unchanged. Since the building walls with finite thermal resistances are not perfect insulators, thermal regulation of radiative heat transfer at exterior FinWall surfaces can affect the indoor environment and save energy consumption for buildings.

Taking Los Angeles as an example, Figure 4B shows the daily energy consumption for the original mid-rise apartment buildings with vertical high-E walls or low-E walls and the dynamic FinWall-integrated buildings in the cooling mode (θ = 75°) and heating mode (θ = 165°). The high-E surfaces and low-E surfaces are defined with thermal emissivities of 0.95 and 0.05, respectively, in EnergyPlus. The energy consumption refers to the heating, ventilation, and air conditioning (HVAC) system in the buildings, namely heating, cooling, and fan energy as provided by EnergyPlus. It is evident that the low-E walls and the heating mode of FinWall consume the least energy on days 1–160 and 300–360, which are relatively cold days in Los Angeles. Conversely, the cooling mode of the FinWall performs better on hot days 180–260 from July to mid-September. This means that the dynamic FinWall is better than both high-E and low-E walls throughout the year. Therefore, the building simulations once again demonstrate that the FinWall design can achieve all-season thermal regulation.

To understand the energy impact of FinWalls in different climate zones, 16 representative cities in the 16 climate zones of the US are chosen, respectively, ranging from a tropical monsoon climate to a subarctic climate. Their angle-optimized annual HVAC energy savings is plotted in Figures 4C and 4D. In the dynamic FinWall case, we use the optimal geometric angle θ on each day in each city to calculate the overall energy savings (Figure S11). The results in Figure 4C indicate that the dynamic FinWall-integrated building always saves energy compared to buildings with high-E walls due to its thermal regulation capability. On average, the dynamic FinWalls save ~221 GJ/year (Figure 4C), or ~24% HVAC energy (Figure 4D), compared to common high-E

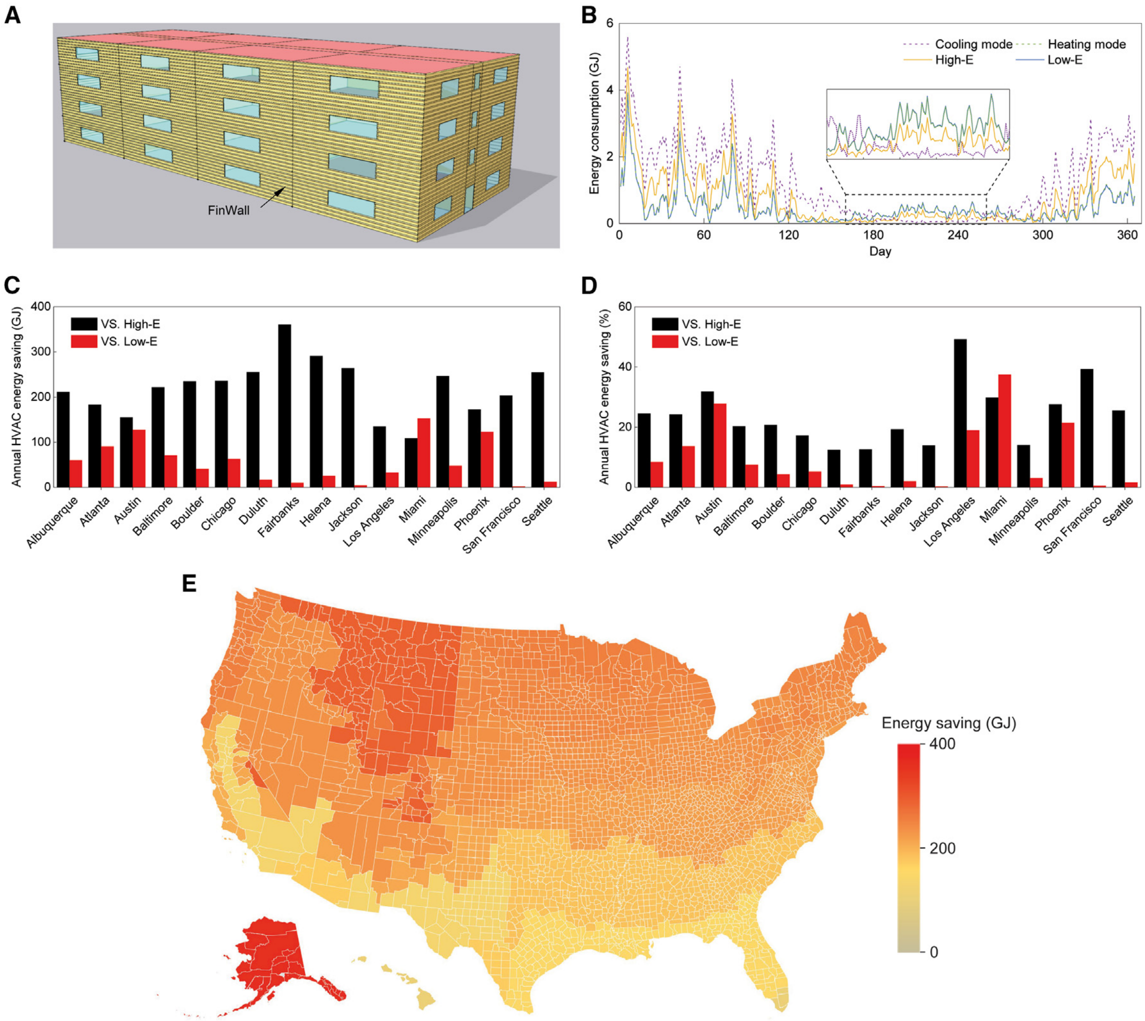

Figure 4. Energy impact of FinWalls

(A) The structure of a mid-rise apartment building integrated with FinWalls.

(B) Daily HVAC energy consumption of the mid-rise apartment building in Los Angeles. HVAC includes heating, cooling, and fan.

(C and D) Annual HVAC energy savings and percentage of the mid-rise apartment buildings with dynamic FinWalls compared to high-E walls and low-E walls in 16 cities in the US. Each city represents a climate zone in the US.

(E) An annual HVAC energy savings map of the FinWall-integrated mid-rise apartment building as compared to the same building with high-E walls.

walls. In addition, the annual energy savings of FinWalls versus high-E walls is mapped in Figure 4E.

On the other hand, the dynamic FinWalls provide more savings than low-E walls in cities with weather conditions similar to or warmer than Chicago, Illinois (e.g., Baltimore, Maryland; Boulder, Colorado; and Miami, Florida, all in the US) but show similar performance to low-E walls in the coldest cities (e.g., Duluth, Minnesota; Fairbanks, Arkansas; and Helena, Montana, all in the US) because buildings in cold cities mostly need a low-E appearance to switch off radiative heat exchange and retain warmth. The average HVAC energy savings of FinWalls versus low-E walls is ~55 GJ/year (Figure 4C), or ~10% (Figure 4D). Generally speaking, the dynamic FinWalls can save ~24% HVAC energy compared to common high-E walls and ~10% compared to low-E walls, highlighting the remarkable potential of the FinWall design for real-world implementation. Furthermore, the HVAC energy savings of FinWalls at a building-to-building distance of 10 m is still 74%–76% effective compared to the standalone case in Baltimore, Maryland (Note S6; Figure S12), which justifies the feasibility of FinWalls in cities where buildings are surrounded by other buildings.

DISCUSSION

A dynamic FinWall design featuring rotatable fin structures was proposed to induce tunable angular LWIR emissivity on the wall surface and achieve all-season thermal regulation. Therefore, in the cooling mode, the FinWall with asymmetric emissivity can reflect terrestrial thermal radiation and retain radiative cooling for hot weather. In the heating mode, it has a low-E appearance to minimize radiative heat exchange for cold weather. The excellent thermal regulation performance was demonstrated through thermal simulations, field tests, and building-scale simulations. This FinWall structure can be easily integrated with conventional wall surfaces by adding a simple revolving joint, and this design can be automated by incorporating a motor. A previous study[31] has proven the feasibility of using motors in smart building envelopes with automatic control. The motor-driven dynamic FinWall consumes only a marginal energy input to rotate fins to the desired angle and lock them in place, and the operation frequency can be adjusted based on weather conditions, ranging from several times a day to once every several days or weeks. If the fin orientation is adjusted daily, then the annual energy consumption of fin movement is on the order of 0.1 MJ, which is negligible compared to the HVAC energy savings that FinWalls bring. This scalable FinWall design demonstrates a simple and feasible approach toward smart and energy-efficient buildings.

EXPERIMENTAL PROCEDURES

Resource availability

Lead contact

Requests for further information and resources and reagents should be directed to and will be fulfilled by the lead contact, Yuan Yang (yy2664@columbia.edu).

Materials availability

This study did not generate new unique reagents.

Data and code availability

All data are available in the manuscript or the supplemental information. This paper does not report original code. Correspondence and requests for materials should be addressed to the lead corresponding author, Yuan Yang.

FinWall fabrication

The LWIR reflective material is a low-cost, ~50-μm-thick aluminized mylar film. The LWIR emissive material is a mylar film coated with PDMS (Sylgard 184). The base and the curing agent were mixed with a 10:1 weight ratio, degassed, drop cast on the reflective mylar film, and cured at room temperature for 3 days. The cured PDMS thickness is ~70 μm. Both the reflective film and the emissive film maintain high optical specularity (Figure S7). Subsequently, they were then cut to size by blade, affixed to aluminum sheets (~0.8 mm thick), and assembled on an acrylic sheet (McMaster-Carr 8560K174) to create the FinWall samples.

Optical measurements

The total reflectance (ρ_{total}) and diffuse reflectance (ρ_{diff}) were determined using integrating sphere setups with angles of incidence set at 30° and 0°, respectively. Two setups (SuperK Extreme laser with Fianium LLTF contrast, Bruker Vertex 70v FTIR) were used to obtain reflectance spectra within three wavelength bands: 0.35–1.1, 1.1–2.5, and 2.5–15.4 μm. The spectra data were later patched together. The specular reflectance ρ_{spec}, specularity, and emissivity ε were calculated using the following equations. I_{bb} is spectral blackbody radiance (Planck's law) at temperature T (assumed to be 20°C).

$$\rho_{spec}(\lambda) = \rho_{total}(\lambda) - \rho_{diff}(\lambda) \quad \text{(Equation 1)}$$

$$\text{specularity}(\lambda) = \frac{\rho_{spec}(\lambda)}{\rho_{total}(\lambda)} \quad \text{(Equation 2)}$$

$$\varepsilon_{\lambda_1 \text{ to } \lambda_2}(T) = \frac{\int_{\lambda_1}^{\lambda_2} I_{bb}(\lambda, T)[1 - \rho_{total}(\lambda)]\, d\lambda}{\int_{\lambda_1}^{\lambda_2} I_{bb}(\lambda, T)\, d\lambda} \quad \text{(Equation 3)}$$

Field tests

Field tests were conducted to demonstrate the FinWall's capability for all-season thermal regulation. The tests were carried out on May 23, 2023, in Queens, New York, USA (40°43′24.7″N, 73°51′10.8″W). Three FinWall samples and a high-E control were vertically mounted on a box facing south, and the box was covered with aluminum foil. Each sample was equipped with a thermocouple (Omega 5TC-TT-K-30-72) at its back surface, sealed with polystyrene foam (McMaster-Carr 93475K63) as thermal insulation, to measure its temperature variation. Additionally, one thermocouple was placed inside the box to measure the ambient air temperature, and another was positioned on the ground to measure the ground surface temperature. A pyranometer (Apogee SP-510) was vertically mounted to measure the solar irradiance onto the wall samples.

SUPPLEMENTAL INFORMATION

Supplemental information can be found online at https://doi.org/10.1016/j.xcrp.2024.101934.

ACKNOWLEDGMENTS

We thank Ms. Guiqin Chen in Queens, New York, for providing the site to carry out the field tests. Y.Y. acknowledges support from the National Science Foundation (award no. 2005747) and the Urban Tech Award at Columbia University.

AUTHOR CONTRIBUTIONS

Y.Y. and Q.C. conceived the idea. Q.C. performed the simulations, prepared the samples, and conducted the experiments. C.T., D.L., and S.T. helped with sample preparation and field tests. M.P. and C.T. helped with EnergyPlus simulations. D.L. helped with COMSOL simulations. Q.C. and Y.Y. supervised the project. All authors contributed to the writing of the paper.

DECLARATION OF INTERESTS

The authors declare no competing interests.

Received: January 8, 2024
Revised: February 29, 2024
Accepted: March 27, 2024
Published: April 19, 2024

REFERENCES

1. (2021). Net-zero carbon pledges must be meaningful to avert climate disaster. Nature *592*, 8. https://doi.org/10.1038/d41586-021-00864-9.

2. U.S. Energy Information Administration (2022). Monthly Energy Review: October 2022. https://www.eia.gov/totalenergy/data/monthly/previous.php.

3. Bloomberg (2023). In a Warming World, 10 Air Conditioners Are Sold Every Second. https://www.bloomberg.com/news/articles/2023-05-17/how-much-air-conditioning-will-it-take-to-cool-the-world.

4. Granqvist, C.G., and Hjortsberg, A. (1981). Radiative cooling to low temperatures: General considerations and application to selectively emitting SiO films. J. Appl. Phys. *52*, 4205–4220. https://doi.org/10.1063/1.329270.

5. Li, D., Liu, X., Li, W., Lin, Z., Zhu, B., Li, Z., Li, J., Li, B., Fan, S., Xie, J., and Zhu, J. (2021). Scalable and hierarchically designed polymer film as a selective thermal emitter for high-performance all-day radiative cooling. Nat. Nanotechnol. *16*, 153–158. https://doi.org/10.1038/s41565-020-00800-4.

6. Li, T., Zhai, Y., He, S., Gan, W., Wei, Z., Heidarinejad, M., Dalgo, D., Mi, R., Zhao, X., Song, J., et al. (2019). A radiative cooling structural material. Science *364*, 760–763. https://doi.org/10.1126/science.aau9101.

7. Mandal, J., Fu, Y., Overvig, A.C., Jia, M., Sun, K., Shi, N.N., Zhou, H., Xiao, X., Yu, N., and Yang, Y. (2018). Hierarchically porous polymer coatings for highly efficient passive daytime radiative cooling. Science *362*, 315–319. https://doi.org/10.1126/science.aat9513.

8. Zhai, Y., Ma, Y., David, S.N., Zhao, D., Lou, R., Tan, G., Yang, R., and Yin, X. (2017). Scalable-manufactured randomized glass-polymer hybrid metamaterial for daytime radiative cooling. Science *355*, 1062–1066. https://doi.org/10.1126/science.aai7899.

9. Raman, A.P., Anoma, M.A., Zhu, L., Rephaeli, E., and Fan, S. (2014). Passive radiative cooling below ambient air temperature under direct sunlight. Nature *515*, 540–544. https://doi.org/10.1038/nature13883.

10. Zhou, L., Song, H., Liang, J., Singer, M., Zhou, M., Stegenburgs, E., Zhang, N., Xu, C., Ng, T., Yu, Z., et al. (2019). A polydimethylsiloxane-coated metal structure for all-day radiative cooling. Nat. Sustain. *2*, 718–724. https://doi.org/10.1038/s41893-019-0348-5.

11. Zhao, D., Aili, A., Yin, X., Tan, G., and Yang, R. (2019). Roof-integrated radiative air-cooling system to achieve cooler attic for building energy saving. Energy Build. *203*, 109453. https://doi.org/10.1016/j.enbuild.2019.109453.

12. Zou, H., Wang, C., Yu, J., Huang, D., Yang, R., and Wang, R.J.C.R.P.S. (2023). Eliminating greenhouse heat stress with transparent radiative cooling film. Cell Rep. Phys. Sci. *4*, 101539. https://doi.org/10.1016/j.xcrp.2023.101539.

13. Heo, S.-Y., Lee, G.J., Kim, D.H., Kim, Y.J., Ishii, S., Kim, M.S., Seok, T.J., Lee, B.J., Lee, H., and Song, Y.M. (2020). A Janus emitter for passive heat release from enclosures. Sci. Adv. *6*, eabb1906. https://doi.org/10.1126/sciadv.abb1906.

14. Ly, K.C.S., Liu, X., Song, X., Xiao, C., Wang, P., Zhou, H., and Fan, T. (2022). A Dual-Mode Infrared Asymmetric Photonic Structure for All-Season Passive Radiative Cooling and Heating. Adv. Funct. Mater. *32*, 2203789. https://doi.org/10.1002/adfm.202203789.

15. Hsu, P.-C., Liu, C., Song, A.Y., Zhang, Z., Peng, Y., Xie, J., Liu, K., Wu, C.-L., Catrysse, P.B., Cai, L., et al. (2017). A dual-mode textile for human body radiative heating and cooling. Sci. Adv. *3*, e1700895. https://doi.org/10.1126/sciadv.1700895.

16. Peng, Y., Chen, J., Song, A.Y., Catrysse, P.B., Hsu, P.-C., Cai, L., Liu, B., Zhu, Y., Zhou, G., Wu, D.S., et al. (2018). Nanoporous polyethylene microfibres for large-scale radiative cooling fabric. Nat. Sustain. *1*, 105–112. https://doi.org/10.1038/s41893-018-0023-2.

17. Zhou, J., Chen, T.G., Tsurimaki, Y., Hajj-Ahmad, A., Fan, L., Peng, Y., Xu, R., Wu, Y., Assawaworrarit, S., Fan, S., et al. (2023). Angle-selective thermal emitter for directional radiative cooling and heating. Joule *7*, 2830–2844. https://doi.org/10.1016/j.joule.2023.10.013.

18. Cheng, Q., Gomez, S., Hu, G., Abaalkhail, A., Beasley, J., Zhang, P., Xu, Y., Mandal, J., Raman, A., and Yu, N. (2023). A Zigzag Wall with Asymmetric Emissivity for Radiative Cooling Building Envelope. Preprint at engrXiv. https://doi.org/10.31224/3283.

19. Mandal, J., Mandal, S., Brewer, J., Ramachandran, A., and Pattabhi Raman, A. (2020). Radiative Cooling and Thermoregulation in the Earth's Glow. Preprint at arXiv. https://doi.org/10.48550/arXiv.2006.11931.

20. Baniassadi, A., Sailor, D.J., and Ban-Weiss, G.A. (2019). Potential energy and climate benefits of super-cool materials as a rooftop strategy. Urban Clim. *29*, 100495. https://doi.org/10.1016/j.uclim.2019.100495.

21. Cohen, J.E., and Small, C. (1998). Hypsographic demography: The distribution of human population by altitude. Proc. Natl. Acad. Sci. USA *95*, 14009–14014. https://doi.org/10.1073/pnas.95.24.14009.

22. Tang, K., Dong, K., Li, J., Gordon, M.P., Reichertz, F.G., Kim, H., Rho, Y., Wang, Q., Lin, C.-Y., Grigoropoulos, C.P., et al. (2021). Temperature-adaptive radiative coating for all-season household thermal regulation. Science *374*, 1504–1509. https://doi.org/10.1126/science.abf7136.

23. Li, J., Dong, K., Zhang, T., Tseng, D., Fang, C., Guo, R., Li, J., Xu, Y., Dun, C., Urban, J.J., et al. (2023). Printable, emissivity-adaptive and albedo-optimized covering for year-round energy saving. Joule *7*, 2552–2567. https://doi.org/10.1016/j.joule.2023.09.011.

24. Wang, S., Jiang, T., Meng, Y., Yang, R., Tan, G., and Long, Y. (2021). Scalable thermochromic smart windows with passive radiative cooling regulation. Science *374*, 1501–1504. https://doi.org/10.1126/science.abg0291.

25. Mandal, J., Du, S., Dontigny, M., Zaghib, K., Yu, N., and Yang, Y. (2018). Li4Ti5O12: A Visible-to-Infrared Broadband Electrochromic Material for Optical and Thermal Management. Adv. Funct. Mater. *28*, 1802180. https://doi.org/10.1002/adfm.201802180.

26. Sui, C., Pu, J., Chen, T.-H., Liang, J., Lai, Y.-T., Rao, Y., Wu, R., Han, Y., Wang, K., Li, X., et al. (2023). Dynamic electrochromism for all-season radiative thermoregulation. Nat. Sustain. *6*, 428–437. https://doi.org/10.1038/s41893-022-01023-2.

27. Xia, Z., Fang, Z., Zhang, Z., Shi, K., and Meng, Z. (2020). Easy Way to Achieve Self-Adaptive Cooling of Passive Radiative Materials. ACS Appl. Mater. Interfaces *12*, 27241–27248. https://doi.org/10.1021/acsami.0c05803.

28. Yin, H., Zhou, X., Zhou, Z., Liu, R., Mo, X., Chen, Z., Yang, E., Huang, Z., Li, H., Wu, H., et al. (2023). Switchable Kirigami Structures as Window Envelopes for Energy-Efficient Buildings. Research *6*, 0103. https://doi.org/10.34133/research.0103.

29. Liu, Y., Tian, Y., Liu, X., Chen, F., Caratenuto, A., and Zheng, Y. (2022). Intelligent regulation of VO2-PDMS-driven radiative cooling. Appl. Phys. Lett. *120*, 171704. https://doi.org/10.1063/5.0089353.

30. Mandal, J., Jia, M., Overvig, A., Fu, Y., Che, E., Yu, N., and Yang, Y. (2019). Porous Polymers with Switchable Optical Transmittance for Optical and Thermal Regulation. Joule *3*, 3088–3099. https://doi.org/10.1016/j.joule.2019.09.016.

31. Lin, Q., Zhang, Y., Mieghem, A.V., Chen, Y.-C., Yu, N., Yang, Y., and Yin, H. (2020). Design and experiment of a sun-powered smart building envelope with automatic control. Energy Build. *223*, 110173. https://doi.org/10.1016/j.enbuild.2020.110173.